Human Intelligence Forming in the Rhythm of Solar Activity

Viktor P. Vasylyev

SVV Technology Innovations, Inc., 1832 Tribute Road, Suite C, Sacramento, CA, USA

e-mail: vicv@svvti.com https://orcid.org/0009-0009-8360-2958

This is a Preprint (version 2) submitted to EarthArXiv and has not been peer reviewed.

Version 2 contains minor but important additions and changes, including consideration of references to new relevant publications. This updated version of the article was not submitted to peer-reviewed journals mainly due to its extremely broad multidisciplinary scope, encompassing environmental biology, Earth's atmospheric physics, solar activity physics, cosmic rays, nuclear physics, radioastronomy, and radiative acoustics.

Abstract

This multidisciplinary study examines a possible link between atmospheric radiation environment, modulated by space weather, and human cognitive development by analyzing correlations of solar activity phenomena with various indicators of intellectual potential. A novel metric, the Proton Flare Index (PFI), is introduced to quantify the influence of high-energy solar proton events on the terrestrial atmospheric environment. Using systemic comparative analysis across interdisciplinary datasets, a strong correlation ($r = 0.98$) was identified between the number of Nobel laureates born and the ratio of the cumulative magnitude of powerful Forbush decreases to the PFI, averaged over three 4-year intervals, adjusted for a six-month prenatal offset. A similar pattern ($r = 0.76$) was observed in the positive and negative trends of average population IQ (the Flynn effect), based on known intelligence tests, conducted over the several decades in different countries. In both cases, no meaningful associations were found when not adjusted for prenatal timing and with conventional sunspot-based solar cycle data. These findings suggest that atmospheric radiation patterns, induced by specific solar and galactic cosmic rays, may act as environmental stressors affecting neural circuit formation during prenatal development. While the precise biological mechanisms remain unclear, such correlations provide a preliminary foundation for rethinking the influence of space weather on human neurodevelopment. In addition to forecasting IQ trends for birth cohorts from 1992 to 2017, the paper explores potential additional contributions to environmental biological effects by secondary particle cascades in the atmosphere, which originate from galactic cosmic rays. This interdisciplinary framework invites further investigations into the role of space-environmental factors in shaping human intelligence, as suggested in the paper.

Keywords: environmental biology, human intelligence, neural development, Earth's radiation background, space weather, solar modulation

1. Introduction

Starting with the pioneering works from the past century (Douglass, 1919; Chizhevsky, 1936), researchers have addressed the interdisciplinary challenge of quantifying how space weather phenomena, including solar activity (SA), temporally modify the Earth's atmospheric environment and influence biological systems. In particular, in the recent work (Nasirpour et al., 2021), in addition to the results of (Chizhevsky, 1936), it is shown that the world’s main pandemics occurred in sunspot number relative extrema, both in maxima and minima. The annual numbers of human births in different countries regarding an eleven-year solar cycle during a long period were analyzed in (Randall & Moos,1993), where 11-year rhythms and correlations with

sunspots, solar flares and some terrestrial disturbances were found. Most works have focused on the use of tree rings as an indicator of the background ionizing radiation (BIR) and the long-lived ^{10}Be and ^{14}C radionuclides conserved in them has become one of the popular probes of this problem. The results from this research suggest that the concentration of radionuclides is correlated with the periodicity of SA rhythm – see (Brehm et al., 2021) and references therein.

On average, up to half of the natural BIR value (around 0.87 mSv/yr) is produced by cosmic radiation from space (around 0.39 mSv/yr) – galactic cosmic rays (GCRs) and solar cosmic rays (SCRs) (United Nations Scientific Committee, 2010). The properties and mechanisms of interaction among GCRs and SCRs with the Earth's atmosphere, as well as their participation in the formation of BIR, have been studied in sufficient detail by now – see, for example, (Mertens et al., 2012; Kampert & Watson, 2012; Potgieter, 2013; Meier et al., 2020) and references therein. SCRs and GCRs with particle energies orders of magnitudes higher than SCRs (but less than 10^{13} eV) create many relatively long-lived radionuclides in the upper Earth's atmosphere. These radionuclides are then distributed globally by geostrophic wind as they settle on the Earth's surface, in particular, due to gravity and clumping with aerosols, including cosmic dust. As a result, they become potentially capable of producing adverse ionizing radiation effects on living organisms at the cellular and molecular levels.

At the same time, being initially constant, this GCR flux is modulated by frequent SA events – Forbush decreases (FDs) – see (Potgieter, 2013) and references therein. These modulations have durations from hours to months and are regulated by the impact of sporadic ejections of solar plasma and recurrent flows of high-speed solar wind, which are also one of the most powerful manifestations of SA rhythm. The weak geomagnetic field practically does not affect most of the above processes due to the high energies of GCR and SCR protons from relativistic flares.

At energies around 10^{14} eV and more, GCRs are capable of creating powerful atmospheric particle cascades - «extensive (extended) air showers» (EAS) – see (Kampert & Watson, 2012) and references therein. Furthermore, the GCR particle flux is isotropic and continuous, unlike the SCR. Primary GCR ions of somewhat lower energies are also capable of triggering nuclear reactions and creating cascades of secondary particles similar to showers in Earth's atmosphere. However, they are likely not powerful enough to clearly fall into the "extensive" category. Recent measurements of secondary particles fluxes also provide evidence that modulations by SA are subject to the GCRs even for primary energies near 2 x10^{13} eV (Agostini et al., 2019; Maghrabi et al., 2021), which is relatively close to those generally considered as sufficient for EAS production. Therefore, this result indicates a modulation of the occurrence rate of EAS. The secondary muon flux dominates the other hadronic-interaction products of the EAS at sea level, potentially affecting biological processes at sea level (Atri & Melott, 2014). This feature is exacerbated by their high penetration ability, allowing them to be used, in particular, for human radiography (Morris et al., 2021).

The brains of animals can be classified as one of the most complex biostructures. Previous works have shown that the consequences of exposure to the brain at low doses of ionizing radiation are of great importance as a health risk – see, for example, (Lowe et al., 2009). This negative effect is manifested, among other things, by a significant influence on the origin and formation of the brain which are associated

with the emergence and development of human neural circuits underlying intelligence (Korr et al., 2001). Note here that the development of neural circuits begins during the first months of the prenatal period with the completion of one of the key stages by its last month (Tau & Peterson, 2010). The influence of SA on the human brain, as well as the general relationship between BIR and extraterrestrial factors with human health, remains an open ended and still somewhat controversial problem, which requires detailed research and analysis. Nevertheless, many works in this field have been published – see the comprehensive review (Zenchenko & Breus, 2021). As follows from the review, most studies conducted so far have traditionally been limited to searching for links between human health and solar-driven disturbances of the geomagnetic field. However, their amplitudes are generally significantly smaller even compared to the Hz-periodic variations of the magnetic field that are constantly produced inside public electric transport (Orlyuk et al., 2020), which are used daily by very large numbers of people without evident harmful effects. Moreover, measurements of physiological parameters are often carried out directly during the period of such solar-driven disturbances without sufficient statistics and with the help of electrical instruments, whose own sensitivity to the SA is not excluded. On the other hand, detailed studies of the possible effects of radiation exposure caused by space weather on mental health are practically absent, while a recent study (Yun et al., 2024) shows that exposure to GCRs may have long-term negative effects on the cognitive health of rodents.

Following from the facts and properties of the phenomena discussed above, it can be assumed that complex biological structures, such as the human brain, may have relatively high sensitivity to changes in the Earth's BIR. It should be emphasized that, given the rarity of powerful relativistic solar proton flares capable of generating SCR, their peak contribution to BIR far exceeds average annual levels. Consequently, during the relatively short lifetimes, on the order of several dozen days, of certain cosmogenic radionuclides, such as ^{7}Be, ^{58}Co, ^{56}Co, ^{46}Sc, ^{48}V, and ^{35}S, the potential radiation impact of this space-weather factor on forming neural circuits may also be much stronger than that of the underestimated annually averaged terrestrial component of BIR.

At the same time, the brain, unlike simple bio-organisms and their parts, adapted sufficiently over its evolutionary history, reducing its dependence on dramatically changing local terrestrial factors such as climate and weather. An exception to this trend can be made for viruses following the results of (Nasirpour et al., 2021). Within this paradigm, it is natural to expect that space weather events, which cause variations in BIR (as a partially space-generated basic radiative component of the global environment), will modulate not only the annual numbers of human births (Randall & Moos, 1993), but also brain development, particularly the formation of neural circuits. Whereas a specific birthday for the human brain is only a time marker for our purposes, since, as noted above, the key development of neural circuits occurs during the prenatal period.

Some of the most prominent representatives of individuals with outstanding intelligence are Nobel Laureates (NLs) (as a global phenomenon), about whom there is long-term and publicly available information. The rest of the dataset, which is necessary in the framework of systemic-analytical methodology, is also available and reflected in the subsequent paragraphs of the article. Further this work is devoted mainly to systemic comparative analysis of space weather data together with the time distribution

of NL births and with global prolonged fluctuations of the mean IQ score for large populations, in order to search for possible influence of secondary ionizing radiation on the forming of their intelligence.

It should be noted that a similar attempt at finding necessary correlations was made several decades ago (Vinogradov, 1989) on a more extensive but more heterogeneous biographical dataset including various celebrities, as well as using outdated, incomplete data on SA. However, since this publication contains a rather problematic description, lacking a rigorous approach, illustrations of results, as well as any references, this does not allow its use in the analysis here. Furthermore, it's important to note that correlation alone does not establish causation. For example, a formal correlation exists between the normalized number of NLs and a seemingly unrelated factor, such as chocolate consumption in different countries. As shown in (Aloys, 2020), this correlation can exist even if there is no connection between these phenomena when the analysis lacks a systemic approach.

2. Results and discussion

Here, to maintain a more homogenous data set for this analysis, a dataset of all NLs until 2024 inclusive awarded only in the fields of sciences (including economics) and literature is chosen from (The Official Website of the Nobel Prize). For an averaged comparison over 11-year cycles N 6 – 20 during years 1817 – 1974, the revised data of the monthly sunspot number (Clette et al., 2014) was used as an index of the general level of SA. For a more systemic comparison and analysis, an additional dataset from (Shea & Smart, 1990) was used. This dataset contains solar proton flares having a flux over 10 particles $(cm^2\ s\ ster)^{-1}$ above 10 MeV over the last SA cycles in which there is NL birth data. These flares are the main indicators of the most powerful SA events. High energy proton flares (~1 GeV) were also taken into account (Cliver et al., 2020). This data covers the last four cycles, which account for approximately 20% of the available NL birth statistics. FDs data cataloged since 1957 for the subsequent SA cycles is taken from (Catalog of the Forbush-effects, 2020).

2.1. Comparison of average NL's and SA data

The processed data is presented in Fig.1 as a distribution histogram (shown in green) of average annual numbers of NLs depending on lag or lead times of their birth time relative to the nearest absolute monthly (not calendar year) maxima of sunspot number within SA cycles.

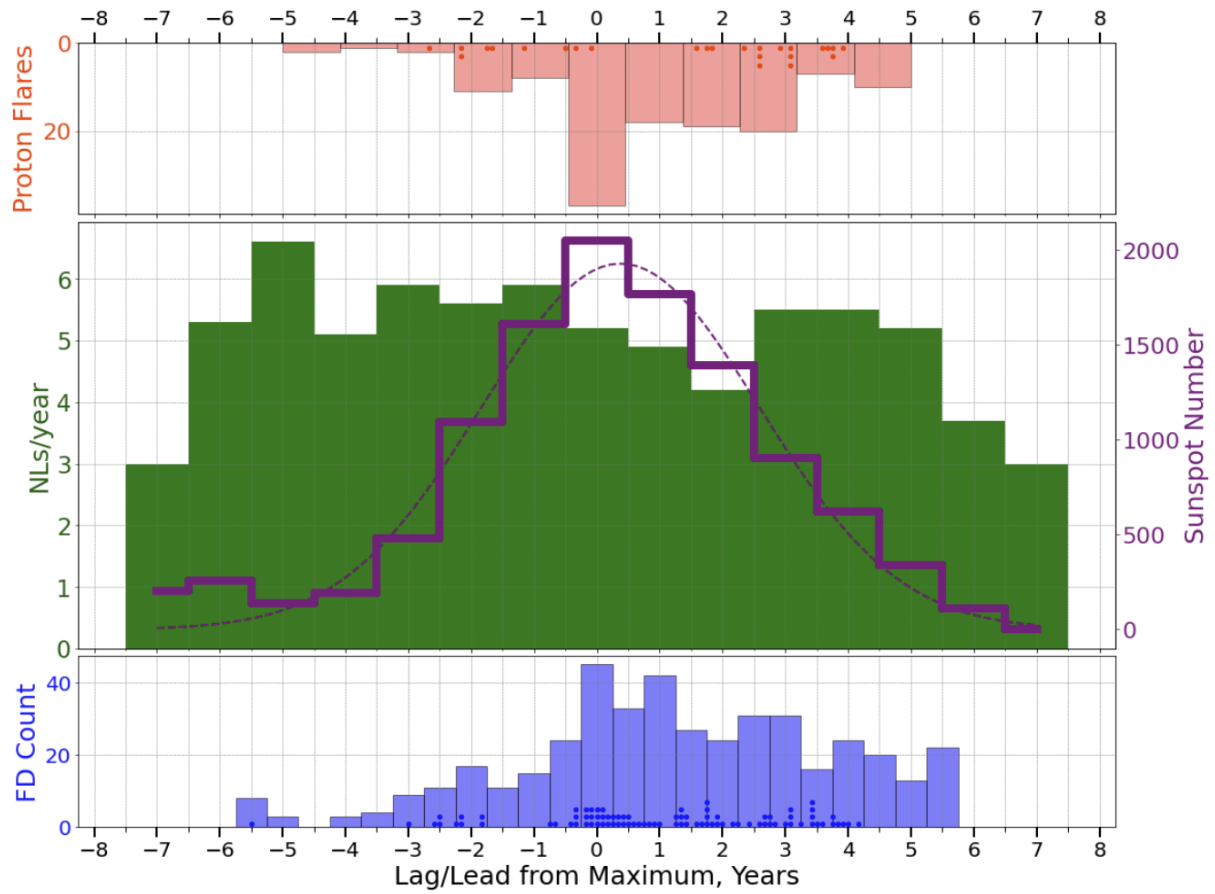


FIG. 1. Comparison of temporal distributions of NL birth rates with solar activity indicators over fifteen 11-year solar cycles. The green histogram shows average annual NL birth rates relative to the year of peak monthly sunspot number in each cycle. Overlaid is the solar activity metacycle (stepped purple line) derived from average annual sunspot numbers (over the fifteen cycles), with a normal distribution fit (dashed purple). Red histogram (top) indicates proton flare occurrences, with large red dots marking relativistic flares. Blue histogram (bottom) shows frequency of FDs with magnitudes 2 – 5, with large blue dots marking FDs ≥ 5. All data are aligned relative to years of peak monthly sunspot numbers within each cycle. Proton flare and FD data cover approximately the last quarter of the full period.

The histogram is overplotted with FD and proton flare occurrences also relative to the SA monthly maximum. The accessibility of the used data allows one, if necessary, to easily verify the results obtained in this work. It is also worth pointing out that all 16 SA cycles used for the analysis vary in duration, in the magnitude of the maximum values (both monthly and annual) of the sunspot number, as well as in the degree of symmetry and smoothness of changes from maximum to minimum (both within a calendar year and within 11-year cycle SA). As a result, the method used here to obtain the distribution of birth times, lagging, and leading periods of the absolute monthly maximum of SA within a cycle should reflect all of the parameters mentioned above even after averaging over all cycles, given that interdependence may exist. Therefore, to estimate the accuracy of this method for a one and a half-century time scale, it is

necessary to compare NL birth frequency to the metacycle, built by averaging the distributions of the annual sunspot number within the considered SA cycles.

The metacycle, constructed following the same averaging procedure as for the histogram, is shown in a purple line on the background of the histogram. The positions of proton flares, both the most powerful ones and those with the above indicated flux values, as well as the powerful FDs, are marked at the top and bottom of Fig.1, respectively. Much less powerful (mag. < 2) FDs are almost uniformly distributed, with approximately 100 events per year. These are not shown in the figure.

As can be seen from Fig.1, the shapes of the histogram and the distribution of SA in the metacycle are quite different. The average annual birth frequency of NLs varies slightly around a mean value of about 5 yr^{-1}, while the corresponding values of the sunspot number vary by up to three orders of magnitude from the marginal (minimum) zones to the central (maximum) peak. We emphasize, however, that these differences, as well as the dissimilarity of the histogram and the metacycle shapes, do not necessarily rule out the dependency of NL births and SA activity. In particular, this may indicate an insufficient use of the existing and rather generalized SA index based purely on sunspot numbers for analysis of solar-terrestrial interconnections.

All FDs selected according to the power criterion, except for one, are concentrated in the zone ± 4 years from the SA maximum (see Fig.1). At the same time, the number of FDs in the post-maximum part of histogram is artificially higher than in the pre-maximum, which may be a consequence of the different number of the full pre-maximum and post-maximum SA half-cycles represented in the existing database for the period under consideration. For relativistic proton flares, this asymmetry is less pronounced. FDs are in general randomly distributed within the pre-maximal and pos-maximal half cycles, with a tendency to increase in frequency near the SA maximum. There are twice as many post-maximal half-cycles considered as compared to pre-maximal ones, resulting in an asymmetric FD distribution overall.

Hence, the average annual frequency of NL births during solar cycles, centered on the monthly maximum of sunspot number, does not change significantly. However, there is an exception for the years of the solar minimum, which go beyond the average duration of some 11-year cycles, meaning we cannot make unambiguous conclusions. Moreover, as noted earlier, the behavior of the general histogram does not match with the normalized metacycle curve based on these same sunspot number data and having a high central peak. Using the cycles with the most abundant data of NLs (14 – 17: 1902 – 1944), we find that the number of NLs born does not show a relationship with the total sunspot number per each cycle. In summary, the number of NLs born changed from cycle to cycle within 15% relative to the mean (NLs ~100). However, the monthly maximum or total sunspot number changed by up to a factor of 2 between cycles.

2.2. Introduction of the PFI for systemic data comparisons

Proton flares are one of the most powerful manifestations of SA rhythm and may play a role as one of the channels for the primary source of atmospheric ionizing radiation that could potentially affect the probability of NL births. In particular, this is indicated by the fact that most of the so-called “pulsed nitrate events” in the polar ice cap, which are generated by exposure to extremely powerful SCR flows (>30 MeV proton fluence > 2 x 10^9 cm^{-2}) during SA cycles 13 – 17 (McCracken et al., 2001) one

year preceding or coinciding with the annual strongest decreases in the NL birth number – see Fig. 2. The annual distributions of NL births and impulsive nitrate events are generally independent of the sunspot number extrema.

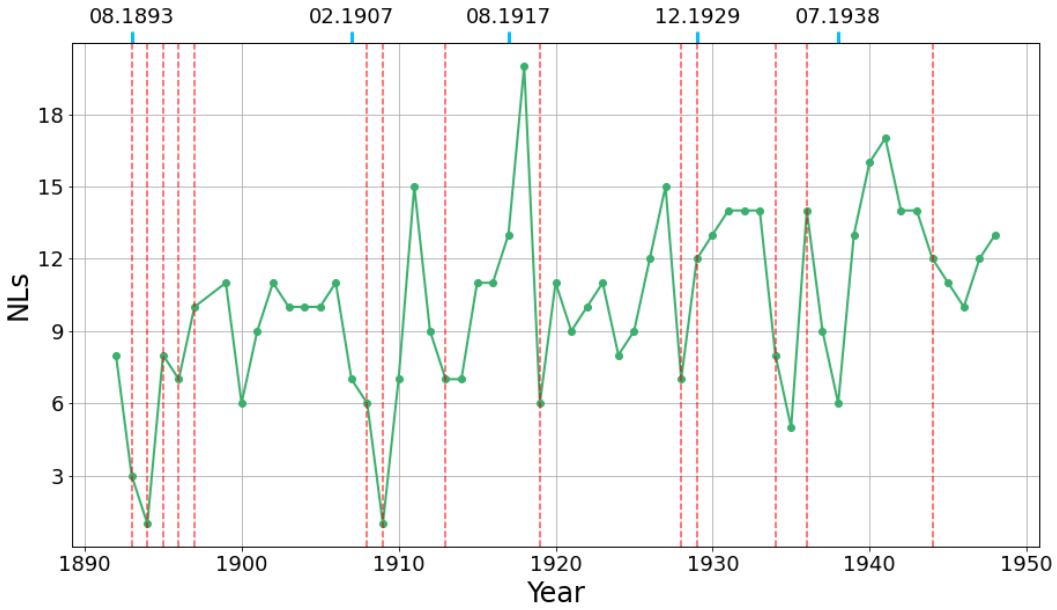


FIG. 2. Annual distribution of NL births during solar cycles 14 – 17, which have the most complete data. The green line represents the number of NL births per year. Red dashed vertical lines indicate the occurrence of impulsive nitrate events, which are generated by powerful SCR streams. Blue tick marks at the top of the figure denote the positions of absolute monthly sunspot number peaks within each solar activity (SA) cycle.

The number of proton flashes by itself may not fully reflect the quantity and properties of BIR radionuclides formed by them in the Earth's atmosphere, since the particle energies in different flashes may differ by at least two orders of magnitude. Therefore, here, for a more accurate comparison and analysis, a quantitative impact index – “Proton Flare Index” is proposed. It is defined by analogy to the sunspot number index (Wolf number): PFI = N_p + 10 N_{pr} , where N_p is the total number of proton flares and N_{pr} is the number of most powerful events among them, where the flux of protons with energy more than 30 MeV is around 10^3 p.f.u. and more, and/or mostly where the proton energy reaches 1 GeV. Since N_{pr}-type flares are quite rare events, summing them over several years is needed to determine the PFI adequate for the purposes of this work.

Another most powerful manifestation of SA is FDs, which significantly modulate the SCR fluxes, occurring mainly in near-maximum periods, as can be seen from Fig.1. Therefore, it is logical to assume that comparison based on the distribution and specific parameters of FDs and proton flares yields the most significant result. However, a more detailed analysis is possible only during a part of the entire period under study – the last three half-cycles (the second half of the 19th and the first half of the 20th cycles (1957 –

1969 years), for which all the necessary data on SA are available (Shea & Smart, 1990; Cliver et al., 2020; Catalog of the Forbush-effects, 2020).

When comparing the values of PFI and the summed magnitudes of FDs, the following should be considered. Firstly, the annual values of the PFI index, constructed according to the data of (Shea & Smart, 1990; Cliver et al., 2020), changed significantly on short timescale (and often asynchronously both with respect to FDs and the variation of the sunspot number) throughout the entire duration of the above half SA cycles. The PFI index changed by as much as sixty units, because these cycles, unlike the previous ones, were anomalously contaminated with relativistic proton flares. Secondly, according to the data of (Catalog of the Forbush-effects, 2020), the number of powerful FDs also changed significantly from zero in the regions of SA minima up to one and a half dozen with their total (summed) magnitude up to more than one hundred near the maximum of the anomalous cycle 19.

Here also, when comparing the data over time, the period of registration of both specified types of space weather events (PFI values and the summarized magnitudes of powerful FDs) must be shifted back by around 0.5 years relative to the real birthdays of NLs (or, if necessary, on the contrary, shift birthdays of NLs forward relative to SA data). The length of the shift was chosen to synchronize the radiation effects with the middle of the prenatal period, taking into account an additional 1.5-month interval sufficient for radionuclides to distribute and reach the near-surface layers of the atmosphere. Since the available data (Catalog of the Forbush-effects, 2020) covered only the second half of 1957, here, for example, the total number of NL births for the period 1958 – 1961 was compared with the ratio FDs/PFI, which is compiled using total data for the second half of 1957, the full years 1958 – 1960 and the first half of 1961. The data for the remaining two intervals were compared in the same way. All these circumstances must also be considered in the study of other helio-biological problems.

For comparison to the PFI, this approach only considered FDs with a magnitude equal to or greater than 4.3 units, which can reflect a significant modulation effect on the GCRs flux. The minimum magnitude taken into account was chosen from the condition of minimizing the number of semi-annual intervals not filled with data about these SA events. The time intervals used to determine the total FD magnitude and the ratio FDs/PFI were shifted 0.5-year back in relation to the 4-year data of NL births. In contrast to the previous case, here, due to the abundance of powerful FDs and proton flares of analyzed period (two SA half-cycles, 1957 –1969 years), the six-month back shift of the SA data (i.e. have been obtained six months prior) relative to the number of NL births allows the use of 4-year intervals even in common with zones of SA minimum. Increasing the number of data summation intervals by shortening them to 3 or 2 years substantially reduces their representativeness due to the small annual numbers of NL births, the need to have the same length of intervals, as well as due to the uneven time distribution of particularly powerful proton flares. The third hemicycle (after 1969) was excluded from consideration due to its extremely weak and intermittent coverage of data on NL births. The latter data which were obtained from (Shea & Smart, 1990; Cliver et al., 2020; Catalog of the Forbush-effects, 2020) in each 4-year interval of the two mentioned SA half-cycles are presented on the histograms of Fig. 3, including cumulative and annual values separately.

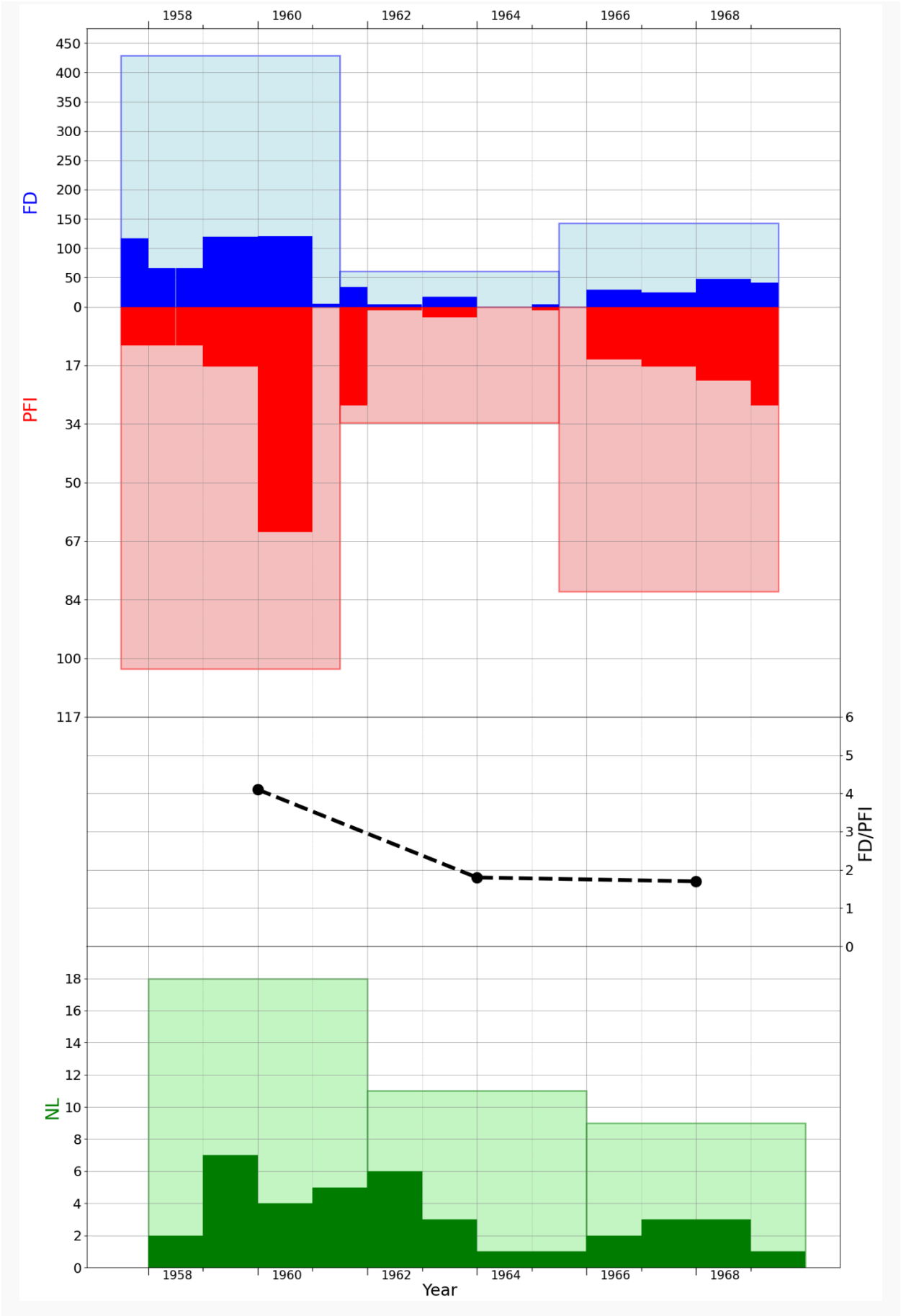

1958
1960
1962
1964
1966
1968
FD
PFI
450
400
350
300
250
200
150
100
50
0
17
34
50
67
84
100
117
FD/PFI
6
5
4
3
2
1
0
NL
18
16
14
12
10
8
6
4
2
0
Year

FIG. 3. Top panel: Data for FDs and PFI are represented separately as combined histograms for both annual and four-year intervals, colored in blue and red respectively. All aggregated SA data are presented for four-year and one-year periods and have been obtained six months prior in relation to the NL birthdays. Middle panel: Ratio of FD to PFI over time, shown as three data points, demonstrating correlation with NL births (bottom panel – distribution of NL births over time).

A strong positive linear connection appears in their ratio: the calculated Pearson's correlation coefficient is 0.98. It is important that here, too, the correlation coefficient becomes insignificant in the absence of a corresponding six-month shift in data. Note also that the correlation coefficient decreases by 1.3 and 1.8 times between NL births and FDs, or NL births and PFI. Meanwhile, the correlation coefficient also decreases by a factor of 1.3 and 1.7 with and without data shift, respectively when comparing NL births with total 4-year sunspot numbers according (Clette et al., 2014). The difference in the extent of the decreases in the correlation coefficient can be considered as an indication of the prevailing role of powerful proton flares among SA events in modulating the number of NL births, similar to the data in Fig. 2. However, a significant correlation exists when comparing NL births to the ratio between FDs and PFI. The inclusion of FDs with a smaller magnitude, the distribution of which relative to the SA maximum is also shown in Fig.1, shows a weak correlation instead.

To further validate the determined correlation, the FDs/PFI ratio was compared for individual NLs whose prenatal periods contained powerful FDs and proton flares to the FDs/PFI ratio averaged over a 12-year period, as shown in Fig. 3. The comparison is performed for only 34 out of 38 NLs, where four cases were excluded due to the absence of proton flares or information about specific birth months in (The Official Website of the Nobel Prize). This comparison, which considered the entire partially overlapping prenatal periods, revealed that the average FDs/PFI ratio for NL-related periods is nearly double the ordinary annual average for the entire 12-year period analyzed. This relationship supports the determined high correlation between NL births and FDs/PFI, suggesting that the SA rhythm during periods of NL neural circuit development is more favorable compared to average conditions.

The result obtained may be attributed to a more trivial explanation. This range is dominated by younger NL’s which represent a subset of the NL population. This is in contrast to the rather homogeneous age distribution in the previously discussed half-cycles (cycles 14 –17). This observation indicates the insufficient filling of these half-cycles with data on the analyzed dates of birth at the moment. According to comparative estimates, this accounts for about half of the total NL population in half-cycles within cycles 14 –17. At the same time, even during this period of final and greatest occupancy (see Fig. 2), 6% of years contain from 1 to 6 NL births. On the other hand, due to the average occupancy of previous periods being close to homogeneity for different age groups, it cannot be ruled out that their future filling will preserve the existing linear correlation within the several-year intervals considered with a possible change in its slope. This interpretation is further supported by the fact that sequentially expanding the dataset with around a third of NL birth dates from the 2023, 2024 and 2025 award years did not lead to an appreciable change in the correlation coefficient. Nevertheless, taking into account the already mentioned lack of complete observational

data on proton flares and FDs for previous years, it can be concluded that the available statistics of all compared data are still insufficient for a definitive conclusion.

Therefore, the obtained result can be interpreted as indication that NL births are dependent on the ratio between the frequency and number of the most powerful SA events – powerful FDs and proton flares, especially relativistic ones. In other words, the emerging patterns and accompanying features are reasonable for the preliminary conclusion that differences in annual birth rates for NLs vary according to the rhythm of SA. Powerful FDs are caused by abrupt changes in GCR intensity via powerful interplanetary shock waves following sporadic solar plasma ejection as well as solar wind disturbances. A definitive conclusion cannot be made here, as the available statistics of these events that coincide in time are still lacking. Future investigation with more complete data on NL births will be important in verifying the preliminary results of this work.

The decline in the NLs birth rate did not occur during major global instabilities, such as war. For example, as can be seen from Fig. 2, the largest annual peaks of NLs births for the entire period under consideration occurred even at the height of the First World War, the Great Depression in the US, and the Second World War, unlike powerful proton flares, which occur (associated with) in the strongest annual decreases. This is consistent with the assumption made above about the predominant sensitivity of complex biostructures to the influence of space weather, standing out against the background of terrestrial negative factors. However, it is possible that due to the low rate at which powerful proton flares occur over the considered timescale, this association is partially due to coincidence. FD data, which would have improved confidence in this result, does not exist for this period.

2.3. Testing the approach with the ratio FDs/PFI

As a test of the approach described in the previous section, it is possible to compare it against a well-known global intelligence phenomenon in which the average IQ scores of a population have risen over time, known as the Flynn effect. A definitive explanation for this effect is still uncertain, especially because the average IQ scores of populations have undergone both increases and decreases globally over decades (Bratsberg & Rogeberg, 2018; Dutton et al., 2016; Flynn, 1987) with the latter referred to as “negative (anti-) Flynn effect”.

To explore possible correlations between IQ and SA rhythm, it is necessary to use IQ scores over extended time intervals, allowing for optimal averaging of data. This requirement arises from the rarity of extremely powerful FDs and proton flares, which play a significant role in determining the PFI value. The primary dataset utilized here is the large-scale, continuous collection of data on IQ score variations for more than half a million young Norwegians, with determined birth years from 1962 to 1991 (Bratsberg & Rogeberg, 2018). Data on powerful FDs of 4.3 units and greater, as well as proton flares for PFI compilation, were sourced from (Shea & Smart, 1990; Cliver et al., 2020; Catalog of the Forbush-effects, 2020). Starting in 1977, modern data on proton flares (NOAA Space Weather Prediction Center), measured by the GOES spacecraft, has been used in this work.

At the same time, the fluence of protons with energies more than 10 MeV is around 10^3 p.f.u. and greater, and were considered as especially powerful events for

constructing the PFI. Given the substantial dataset available for this analysis, it is possible to average annual IQ score data over a short interval (less than 4 years).Therefore, despite the abrupt changes in the annual values of powerful FDs and PFI, data were averaged across various multi-year intervals, without obscuring the discernible trends in changes to IQ scores. Given the absence of specific birth month data for the subjects in reference (Bratsberg & Rogeberg, 2018), this work performs a necessary semi-annual shift back to the SA data relative to the birth year considered.

TABLE 1

Observed birth years	**Total number of people**	**FDs/PFI (synchronous)**	**FDs/PFI (shifted)**	**Average IQ score**
1962 - 1963	58 783	21.6 / 4	38.6 / 30	99.55
1964 - 1967	25 327	58 / 43	80.2 / 44	99.97
1968 - 1869	64 196	107.1 / 62	90 / 60	100.85
1970 - 1973	121 337	142.8 / 76	149 / 77	101.52
1977 - 1979	72 186	150.5 / 48	126 / 44	101.73
1980 - 1982	71 101	191.7 / 64	150.4 / 58	101.20
1983 - 1984	46 330	26.2 / 19	92.2 / 48	100.95
1990 - 1991	54 312	362.7 / 203	245.6 / 160	99.65

Note: Synchronous refers to the absence of a shift of the people's birth years relative to the SA data.

The dynamics between the two-, three- and four-year average IQ scores and FDs/PFI values are shown in Table 1, excluding periods of SA minima without powerful FDs and proton flares. In this case, unlike the situation in the previous sections, equal time intervals are not necessary, allowing them to maximize their number without loss of information near the zones of SA minima. As shown in Table 1, there is a notable trend where the IQ score initially increases and then decreases in tandem with the FDs/PFI ratio. Significantly, one of the SA minima aligns with the peak of the IQ score distribution, suggesting that the intelligence parameters studied are independent of the number of sunspots. Additionally, the period of observed IQ scores from 1962 –1969 overlaps with the finite period discussed in the preceding section. Concurrently, the annual dynamics of NLs births (refer to Fig. 3) and IQ scores show a qualitative agreement, exhibiting an annual variability followed by a rise. These patterns lend further support to the validity of the correlations identified in this study.

The calculated Pearson's correlation coefficient is 0.76, indicating a reasonably strong relationship between the IQ score and the ratio used for the most potent SA events. However, the correlation coefficient is insignificant when comparing FDs and PFI separately as well as when comparing IQ scores (Bratsberg & Rogeberg, 2018) with sunspot numbers (Clette et al., 2014) annually or within intervals of Table 1. In addition, when comparing FDs/PFI with IQ score during the periods of its estimations, i.e.18 years after the births of observed persons, the relation becomes weakly anti-correlated. The correlation coefficient also becomes insignificant unless the birthdays are adjusted forward by shifting the SA data back by six months (see column «synchronous» in the Table 1), similar to the results described in the previous section.

It is noteworthy that these results were obtained even without accounting for the correction of time shift in cases of possible anomalies in the distribution of birthdays within each year, which is not feasible due to the lack of such details in (Bratsberg & Rogeberg, 2018). This uncertainty becomes relevant when using a constant six-month shift, as evidenced by the fact that the correlation coefficient decreases several times when comparing annual IQ scores with corresponding annual SA data for about half of the 30 years (i.e., without averaging over longer intervals) during which powerful FDs and powerful or relativistic proton flares were observed. Therefore, more detailed comparative analyses of this type should take into account at least the months of birth to adjust the position of the SA data shift for more accurate conclusions.

At the same time, according to (Bratsberg & Rogeberg, 2018), there were no local decreases in IQ score in the intervals around two SA minima (1974 –1976 and 1985 -1987), which lacked the powerful FDs and/or powerful proton flares. Therefore, they are not included in the comparative analysis above, in contrast to the previous minimum where this could have been compensated for by using longer intervals. It is essential to consider that up to a hundred weak FDs (mostly with magnitudes less than 2 units), as noted earlier based on (Catalog of the Forbush-effects, 2020), typically remain around the SA minima. They are collectively capable of reducing the GCR flux and its negative impact without competition from proton flares.

The preceding explanation corresponds to the observational data also mutually correlating during the above three-year intervals around SA minima, not included in Table 1. On the one hand, according to (Catalog of the Forbush-effects, 2020), the summed magnitudes of weak FDs during these intervals are 376 and 370 (taking into account the corresponding semi-annual data shifts), which even exceed analogous values for the most powerful FDs during intervals of the same duration. On the other hand, the average IQ scores for these intervals are 102.2 and 100.6, which is close to their absolute and local peaks among the data (Bratsberg & Rogeberg, 2018). These arguments may also be valid in explaining the occurrence of the world's main pandemics around both SA extrema (Nasirpour et al., 2021).

It is crucial to note that when the Flynn effect was initially introduced in (Flynn, 1987) and for some time thereafter, it was referred to as a secular IQ increase in the population of numerous countries. Generally, the selection of initial data for interpreting the results was made without focusing on the determined birth years of the observed individuals, unlike the data in (Bratsberg & Rogeberg, 2018). In some publications, the ages of the observed cohorts were indicated, being outside the several periods around

SA maxima by birth year, or it had been noted that this trend is stronger for adults than children – see references in (Bratsberg & Rogeberg, 2018).
However, as inferred from the tables in Flynn's original article (Flynn, 1987), in cases where it is possible to determine the birth years of observed children with IQ gains in various countries (The Netherlands, Canada, USA, Great Britain, Australia, Japan, Germany, Switzerland), these years partially coincide with the first half of the period used in (Bratsberg & Rogeberg, 2018), where the IQ increased along with the ratio of FDs/PFI.

Regarding the negative (anti-Flynn) effect, a few works referenced in the review (Dutton et al., 2016) provide short-term data on the ages of assessed cohorts, making it possible to determine their birth years. For additional comparison, the results of (Shayer & Ginsburg, 2007) were also used, which demonstrate significant drops in intelligence and abilities of younger schoolchildren (aged 11 to 12) in Great Britain within the testing period from 1995 to 2003. This period overlaps the birth years of the tested children in (Shayer & Ginsburg, 2007) with the data in (Bratsberg & Rogeberg 2018) used earlier, during which there was also a decrease in IQ scores, manifesting the anti-Flynn effect.

According to the review (Dutton et al., 2016), the birth years of residents whose IQ scores were assessed in other countries (Denmark, Finland) for shorter periods using different methods and showed the presence of an anti-Flynn effect also overlap with the birth years in the test used earlier, fitting into a correlation with a decline in the ratio of FDs/PFI. This trend continues, including the period between 1992-1994 of birth data not covered by (Bratsberg & Rogeberg 2018), with FDs/PFI values of 0.16, which is pointed out in (Dutton et al., 2016) towards the anti-Flynn effect obtained in 2012 in Estonia by IQ score testing 18 –19-year-olds.

However, a recent large-scale U.S. study reported that IQ changes "meeting or exceeding the magnitude of a Flynn effect, or its reversal, were not present across the full sample of 18- to 60-year-olds" (Dworak et al., 2023). Despite this overall finding, the Dworak et al. study did observe the largest IQ point decline specifically within the 18- to 22-year-old age group. Notably, the birth years for this cohort, tested early in the 2006–2018 interval, align with the period associated with minimal scores observed in the latter part of the Bratsberg & Rogeberg (2018) testing interval. Furthermore, Dworak et al. (2023) also noted small, divergent year-to-year fluctuations in average IQ scores during their testing period. Within the proposed framework of SA influence, these complex and seemingly contradictory findings—the lack of an overall trend, a decline concentrated in the youngest cohort, and short-term fluctuations—may potentially be reconciled. This perspective suggests that subjects across the wide age range studied by Dworak et al. experienced varied SA conditions during their critical prenatal development periods (corresponding to potentially 'more favorable' or 'less favorable' phases of SA rhythms), which could mask consistent trends when averaged across the entire cohort or lead to specific effects in narrower age groups.

Based on existing data in (Catalog of the Forbush-effects, 2020; NOAA Space Weather Prediction Center), during subsequent three-year intervals, excluding periods around SA minima where powerful FDs and/or powerful proton flares were absent (1992 –1994; 1998 – 2000; 2001 – 2003; 2004 – 2006; 2012 – 2014; 2015 – 2017), FDs/PFI values are determined as 72.9/52; 127.7/58; 231.2/122; 160.8/67; 55,4/77 and 33.6/38, respectively. These SA dynamics can be used in future studies to test the

correlations obtained in this work. It can be expected that the IQ scores of people born within 3-year intervals after observed in (Bratsberg & Rogeberg 2018) (considering the semi-annual shift forward of their birthdays, i.e. within Jul 1992 – Jun 1995, Jul 1998 – Jun 2001 and other corresponding intervals) will increase followed by a significant decrease, correlating with FDs/PFI ratios: 1.4; 2.2; 1.9; 2.4; 0.7 and 0.9.

In summary, the SA-related approach test should be considered insufficiently detailed on a global scale, because the necessary dataset is not yet available despite adequate statistics. For definitive conclusions, targeted global studies of the Flynn and anti-Flynn effects are needed, which are beyond the scope of this work. Nevertheless, this test can be regarded as an additional indication of the influence of the SA rhythm on the probability of NL births, detectable primarily during periods when the most potent SA events occur, as well as an argument for explaining the Flynn and anti-Flynn effects.

2.4. The possible effects of EAS on the human brain

The extremely high energies of GCRs, along with the diverse atmospheric radiation phenomena they generate via continuous global Earth's irradiation, suggest their influence is not limited to BIR contributions. Therefore, the impact of GCRs, capable of generating EASs, on the global environment with possible human health implications should also be analyzed using a systemic approach, which implies consideration of the maximum available number of interrelated processes. As indicated in (United Nations Scientific Committee, 2010), a significant part of the average BIR value induced by cosmic sources is contributed by secondary muons from GCRs. However, the muon flux is concentrated mainly in the EAS cross section at the Earth’s surface (“muon spot”).

The radiation background inside the local area of the “muon spot”, which can cover up to 10^4 m², significantly exceeds the average value of the BIR generated by them. Therefore, although the average muon flux is rather innocuous, the "muon spots" produce a more hazardous radiation value when a human enters their region. As follows from data in (Tanaka, 2022), for a private property with an area 200 m² this is expected to occur in intervals around a day, which carries the potential risk of damaging trillions of DNA as estimated in (de Groen, 2022). Therefore, avoiding repeated entry of any human into the most impactful zone near the axis of the EAS is quite unlikely even in a relatively short prenatal period.

The transverse dimension encompasses only a few meters in the upper region of the EAS to hundreds of meters close to the Earth's surface. These dimensions correspond to observed radio waves in the MHz range (Allan, 1972; Huege, 2016). Meanwhile, the longitudinal dimension covers dozens of kilometers or more, especially if the EAS axis is oriented far from the vertical direction.

An electromagnetic cascade involving the production of electron–positron pairs accompanies the EAS almost along its entire length, owing to muon interactions with solid matter; see references in Kampert & Watson (2012). Therefore, it is likely that pulsed extremely low-frequency radio emission (ELF: 3 Hz–3 kHz) also occurs due to EAS. It is important to emphasize that this type of radio emission, partially observable as Hz-range Schumann resonance — see Nickolaenko et al. (2025) and the review references therein — is generated by conventional lightning, which in turn is stimulated by EAS in areas of electric-charge accumulation, as was recently found by Shao et al.

(2025). In other words, a chain of interdependent phenomena operates in the atmosphere: GCR → EAS → lightning → ELF radio emission. This type of radio emission has also previously been observed from other sources; see Tanaka et al. (2011) and references therein. Importantly, 60 Hz radio emission from a laboratory generator has been experimentally shown to be bioactive, having an adverse effect on the brains of animals (Martínez-Sámano et al., 2018).

As an illustration of the variety of EAS's effects, we note that they are also sources of pulsed flashes of Cherenkov radiation (Watson, 2011), which are generated by secondary electrons that have superluminal speeds in the atmospheric medium. Therefore, the existence of a similar mechanism that stimulates the occurrence of transient luminous events, which are associated with the dynamics of the local properties of the atmosphere (Gordillo-Vázquez & Pérez-Invernón, 2021), cannot be ruled out. In terms of proposed connections, it is important to note that some of these luminous events are also sources of extremely low frequency radio emission (Qin et al., 2012).

Moreover, EAS can additionally generate infrasound, the general bioactivity and negative impact of which on the brain has been actively studied recently - see (Ascone et al., 2021) and their references. In this case, infrasound can occur in the atmosphere due to its local impulse overheating (the so-called "radiative-acoustic" phenomenon) by radiation losses of EAS particles, similar to the "track-breaking" mechanism (Vasylyev et al., 2004) to explain GCRs impact on solids in space. Although the value of this local overheating is not yet known, this assumption is supported by the depth of shower maximum (dozens of meters and more) (Giler et al., 2021), which corresponds to the wavelengths of the infrasound Hz range. Furthermore, according to radiative acoustics, the frequency of generated atmospheric oscillations is determined by the size of the overheated zone, but not by the duration of the overheating pulse - see (Vasylyev et al., 2004) and references therein.

The existence of infrasound produced by EAS in the atmosphere also appears to be quite likely, especially given the detection of a series of narrowband signals ranging from approximately 1 Hz to 22 Hz in the stratosphere that occur a few times per hour (Bowman & Lees, 2015). Later, the authors (Lamb et al., 2018) found a partial coincidence of infrasound signals with lightning discharges, which, taking into account (Shao et al., 2025), may also indicate the role of EAS as their root cause. Additionally, a connection has been found between infrasound detections and one type of transient luminous event, sprites (de Larquier & Pasko, 2010). The similarity of properties between sprites and EAS, such as extremely short duration, localization in the atmosphere, shape, orientation, and size, can also indicate that sprites are stimulated by GCRs, as with conventional lightning in the lower atmosphere (Shao et al., 2025). Further studies are needed to confirm these interconnections. Therefore, if additional bioactive wave phenomena produced by EASs are detected, it will significantly expand our understanding of the impact of space weather on the human brain and its consequences.

3. Limitations

There are several important limitations to this study that warrant consideration. One limitation is that the existing statistics on NL's birth, in contrast to the datasets related to population's IQ score dynamics, are still insufficient to draw definitive conclusions. The main reason for this is that cataloged data on FDs, which are essential for constructing the FD/PFI relationship and subsequently comparing it with NL's births, have only been available since 1957. On the other hand, data on NL's births are also limited in recent years of the period under consideration. Another limitation of the study is that, despite the logical sequence of known events linking space weather phenomena with radiation conditions on Earth's surface, the direct mechanism by which ionizing radiation affects the development of neural circuits during the prenatal period remains unexplored. Therefore, even with the consistent results obtained, the proposed interpretation—developed within the paradigm of a connection between forming intelligence and space weather—should currently be regarded as preliminary and in need of further clarification.

4. Conclusions

Based on the results obtained, the current hypothetical concept that could explain the specific correlations of human intelligence with the dynamics of space weather phenomena is proposed. The human brain is measurably sensitive to the regulation of the Earth's BIR value under the influence of space weather through a sequence of atmospheric phenomena confirmed experimentally. Moreover, such sensitivity manifests itself at the stage of formation and development of neural circuits underlying intelligence, but not synchronously with the state of the space weather during the day of NL's birth or periods of the average IQ score estimations. In this context, the potential implications extend to the entire human population. Initially steady fluxes of GCRs, which significantly contribute to the creation of BIR, are the key stressors, negatively affect the human brain and health in general. These stressors manifest in the Earth's atmosphere, in which both its ionization with the formation of radionuclides and nuclear interactions of the most high-energy GCRs ions occur. Nuclear interactions play a decisive role in driving EAS phenomena with their multiple accompanying atmospheric effects and secondary particles that reach the Earth's surface and even deeper.

Moreover, secondary particles such as muons are capable of locally exerting a much greater influence on the human brain than the average value of BIR. This influence is ensured by the high probability of a human coinciding within the "muon spots", especially near the EAS axis. Meanwhile, proton flares generate episodic fluxes of SCR particles, which in turn contribute to the formation of BIR by the radionuclide production in the atmosphere and therefore act as an additional stressor.

However, SA is capable of affecting the discussed processes in a dual manner according to the diversity of its rhythm, which is instead manifested in the interplanetary environment. FDs, whose magnitude reflects the strength of SA modulation of the GCR flux, act opposite to the effects of GCRs and SCRs, thus functioning as a dynamic "interplanetary shield" for the neural circuit formation.

Even in cases of temporal coincidences in total for several years of both SA phenomena, such as powerful plasma eruptions and proton flares with the latter’s SCRs reaching the Earth's atmosphere, the GCR flux can decrease in strength which in turn reduces the BIR and its accompanying negative impact. However, if the number of

powerful plasma eruptions (measured as powerful FDs) is comparatively small, then conditions are created for an increasing BIR with its negative impact.

Therefore, as a result of this relatively non-trivial superposition of competing impacts from all these transient-type SA phenomena, the probability of more favorable conditions for the birth of intellectually outstanding individuals remains quasi-constant over 11-year solar cycles. However, the probability may decrease during periods of intense proton flares or increase during periods of strong FDs, considering the quantity of atmospheric radionuclides and their dynamics due to varying half-lives. Variations in the IQ scores of the average population behave similarly with the same trends in different countries, not correlating with the SA rhythm during the testing period. Due to cell regeneration and brain adaptation, such an impact may not be severe but is sufficient for noticeable modulation of intelligence against the backdrop of negative terrestrial factors.

At the same time, the similarity in the number of NL births during periods around both SA extrema, determined by the number of sunspots, and the insensitivity of IQ score to the 11-year SA cycle in the Flynn and anti-Flynn effects, can be explained by the "protective" role of up to a hundred weak FDs that remain yearly. During SA minima, they are collectively capable of reducing the GCR flux and its negative impact without competition from proton flares also creating the BIR. In general, periods on Earth that are “more favorable” for the development of human cognitive abilities alternate with “less favorable” ones.

The results obtained should be regarded as preliminary, because the available statistics that coincide in time with all datasets compared, especially regarding the NLs birth rates, are still insufficient to draw definitive conclusions. In other words, more work is required before a definitive association can be made between intelligence forming and space weather phenomena, but these results are a requisite step in proving it to be the case.

5. Future perspectives

Nevertheless, the results obtained can already be considered as a platform for further prospective studies that can contribute to our understanding of the factors shaping human intelligence and cognitive development across populations. These studies are essential for a more comprehensive analysis of the space weather effects on human health, particularly on the brain, both within the Earth's atmosphere and in space.

Primary research areas can include the search for sufficient evidence of global synchronism in the manifestations of positive and negative Flynn effects and their dependence on participant birth dates in relation to the SA rhythm by comparison with the FDs/PFI, taking into account the predictions proposed in this work. In this case, it is advisable to consider not only the year of birth, but also the month or day in order to be able to compare their IQ score with the SA rhythm directly during a time interval, which includes the entire prenatal period. In turn, when testing a cohort with the same birth dates among its members, this will contribute to obtaining more unambiguous results.

Potential negative stressors may include recently detected, not yet explained, but probably EAS-related, Hz-range infrasonic signals. Moreover, they may also include bioactive short-term ELF radio pulses in the Earth's atmosphere, partially observable as lightning-related Schumann resonance, in addition to the well-known MHz radio pulses generated directly by EAS. To validate these hypotheses, a cross-correlation between these phenomena needs to be established. However, as of now, there is no information available about research being conducted in this direction.

It is well known that these types of waves have weak attenuation over planetary distances, and that at least 10^7 EASs occur on earth every second, which may lead to the existence of constant bioactive radio- and infrasonic backgrounds everywhere at the Earth in addition to BIR. Direct or indirect detection of these backgrounds may be aided by their supposed variability depending on SA. Therefore, it is especially important to confirm the modulating effect of SA on primary GCR particles, at least for their minimum energies, at which they can produce EAS.

Beyond that, it would be a useful exercise to compare and systemically analyze global statistics of a wide range of phenomena and incidents in human life – from diseases to car accidents. It is also important to conduct biological experiments on animals at various geomagnetic latitudes and altitudes above sea level to detect and analyze brain responses to the most powerful SA phenomena. In this context, it is possible that the ratio FDs/PFI may turn out to be more universal for searching for dependencies between various properties of living organisms and space weather.

Additionally, there is a dependence on the parameters of solar plasma flows that produce FDs, namely, their type, extent, velocity, density, magnitude of the frozen magnetic field, etc. Correctly considering the influence of these parameters on the modulation effects of FDs, especially for the high-energy component of GCRs, is a separate and rather complicated problem. Therefore, future acquisition of data from direct measurements of all these parameters in the interplanetary medium by spacecraft will be able to specify the roles they play in attenuating GCR flows. Generally, all further steps to clarify the complex space-brain relationships should be based on adopting a holistic and systemic approach.

Data Availability Statement

The data that support the findings of this study are publicly available from:

1. https://www.nobelprize.org/prizes/lists/all-nobel-prizes/
2. http://www.sidc.be/silso/datafiles
3. https://doi.org/10.1007/BF00152170
4. https://doi.org/10.3847/2041-8213/abad44
5. http://spaceweather.izmiran.ru/eng/dbs.html
6. https://doi.org/10.1073/pnas.1718793115
7. https://doi.org/10.1016/j.intell.2016.10.002
8. https://doi.org/10.1037/0033-2909.101.2.171

9.https://www.ngdc.noaa.gov/stp/space-weather/interplanetary-data/solar-proton-events/SEP%20page%20code.html

References

Agostini, M., Altenmüller, K., Appel, S., et al. (2019). Modulations of the cosmic muon signal in ten years of Borexino data. *Journal of Cosmology and Astroparticle Physics*, 02. art. id. 046. doi: 10.1088/1475-7516/2019/02/046

Allan, H. (1972). Low Frequency Radio Emission from Extensive Air Showers. Nature, 237, 384–385. https://doi.org/10.1038/237384a0

Aloys, L.P. (2020). Chocolate consumption and Noble laureates. *Social Sciences & Humanities Open*, 2 (1). https://doi.org/10.1016/j.ssaho.2020.100082

Ascone, L., Kling, C., Wieczorek, J., et al. (2021). longitudinal, randomized experimental pilot study to investigate the effects of airborne infrasound on human mental health, cognition, and brain structure. *Science Reports*, 11, 3190. doi: 10.1038/s41598-021-82203-6

Atri, D., & Melott, A.L. (2014). Cosmic rays and terrestrial life. A brief review. *Astroparticle Physics*, 53,186 – 190. doi:10.1016/j.astropartphys.2013.03.001

Bowman, D.C., & Lees, J.M. (2015). Infrasound in the middle stratosphere measured with a free-flying acoustic array. *Geophysical Research Letter*, 42 (22), 10,010 –10,017. https://doi.org/10.1002/2015GL066570

Bratsberg, B., & Rogeberg, O. (2018). Flynn effect and its reversal are both environmentally caused. *PNAS*, 115 (26), 6674 – 6678. https://doi.org/10.1073/pnas.1718793115

Brehm, N., Bayliss, A., Christl, M., et al. (2021). Eleven-year solar cycles over the last millennium revealed by radiocarbon in tree rings. *Nature Geoscience*, 14, 10 –15. doi: 10.1038/s41561-020-00674-0

Catalog of the Forbush-effects and interplanetary disturbances (2020). IZMIRAN SPACE WEATHER PREDICTION CENTER. http://spaceweather.izmiran.ru/eng/dbs.html

Chizhevsky, A.L. (1976). The terrestrial echo of solar storms, Moscow, 366 pp. (First published in 1936 in Russian).

Clette, F., Svalgaard, L., Vaquero, J.M., et al. (2014). Revisiting the sunspot number. A 400-year perspective on the solar cycle. *Space Science Reviews*, 186 (1 – 4), 35 –103. http://www.sidc.be/silso/datafiles

Cliver, E.W., Mekhaldi, F., & Muscheler, R. (2020). Solar longitude distribution of high-energy proton flares: Fluences and Spectra. *Astrophysical Journal Letter*, 900 (1), id. L11, 1 – 7; https://doi.org/10.3847/2041-8213/abad44

Douglass, A.E. (1919). Climatic cycles and tree-growth, Carnegie Institution, Washington, 127 pp.

Dutton, E., van der Linden, D., & Lynn, R. (2016). The negative Flynn Effect: A systematic literature review. *Intelligence*, 59, 163 –169. https://doi.org/10.1016/j.intell.2016.10.002

Dworak, E.M., Revelle, W., & Condon, D.M. (2023). Looking for Flynn effects in a recent online U.S. adult sample: Examining shifts within the SAPA Project. *Intelligence*, 98, 101734. https://doi.org/10.1016/j.intell.2023.101734

Flynn, J.R. (1987). Massive IQ gains in 14 nations: What IQ tests really measure. *Psychological Bulletin*, 101(2),171–191. https://doi.org/10.1037/0033-2909.101.2.171

Giler, A.G.D., Arbeletche, L.B., Bird, R., et al. (2021). Measuring the depth of shower maximum of extensive air showers using Cherenkov light. *Astroparticle Physics*, 124, 102508. doi: 10.1016/j.astropartphys.2020.102508

Gordillo-Vázquez, F.J., & Pérez-Invernón, F.J. (2021). A review of the impact of transient luminous events on the atmospheric chemistry: Past, present, and future. *Atmospheric Research*, 252, art. id.105432. doi: 10.1016/j.atmosres.2020.105432

de Groen, P.C. (2022). Muons, mutations, and planetary shielding. *Frontiers in Astronomy and Space Science*, 9, 1067491. doi: 10.3389/fspas.2022.1067491

Huege, T. (2016). Radio detection of cosmic ray air showers in the digital era. *Physics Reports*, 620, 1 – 52. doi: 10.1016/j.physrep.2016.02.001

Kampert, K-H., & Watson, A.A. (2012). Extensive air showers and ultra high-energy cosmic rays: a historical review. *European Physics Journal H*, 37(3), 359 – 412. doi:10.1140/epjh/e2012-30013-x

Korr, H., Thorsten Rohde, H., Benders, J., et al. (2001). Neuron loss during early adulthood following prenatal low-dose X-irradiation in the mouse brain. *International Journal Radiation Biology, 77*(5), 567 – 580, PMID 11382335. https://doi.org/10.1080/09553000010028467

de Larquier, S., & Pasko, V.P. (2010). Mechanism of inverted-chirp infrasonic radiation from sprites. *Geophysical Research Letters*, 37(24), Cite ID: L24803. doi:10.1029/2010GL045304

Lamb, O.D., Lees, M. J., Bowman, D.C. (2018). Detecting lightning infrasound using a high-altitude balloon. https://eartharxiv.org/repository/view/1379/

Lowe, X.R., Bhattacharya, S., Marchetti, F., et al. (2009). Early brain response to low-dose radiation exposure involves molecular networks and pathways associated with cognitive functions, advanced aging and Alzheimer's disease. *Radiation Research*, 171(1), 53 – 65, PMID:19138050. doi:10.1667/ RR1389.1

Maghrabi, A., Aldosari, A., & Almutairi, M. (2021). Correlation analyses between solar activity parameters and cosmic ray muons between 2002 and 2012 at high cutoff rigidity. *Advances in Space Research*, 68(7), 2941 – 2952. doi:10.1016/j.asr.2021.05.016

Martínez-Sámano, J., Flores-Poblano, A., Verdugo-Diaz, L., et al. (2018). Extremely low frequency electromagnetic field exposure and restraint stress induce changes on the brain lipid profile of Wistar rats. *BMC Neuroscience*, 19(31), 1 – 9. doi:10.1186/s12868-018-0432-1

McCracken, K.G., Dreschhoff, G.A.M., Zeller, E.J., et al. (2001). Solar cosmic ray events for the period 1561-1994 1. Identification in polar ice, 1561-1950. *Journal of Geophysical Research*, 106 (A10), 21585 – 21598. doi: 10.1029/2000JA000237

Meier, M.M., Copeland, K., Kloeble, K., et al. (2020). Radiation in the atmosphere - a hazard to aviation safety? *Atmosphere*, 11(1358), 1 – 31. doi:10.3390/atmos11121358

Mertens, C.J., Kress, B.T., Wiltberger, M., et al. (2012). Atmospheric Ionizing Radiation from Galactic and Solar Cosmic Rays In: Nenoi M (ed.) *Current topics in ionizing radiation research*, pp. 683 – 738. doi: 10.5772/32664

Morris, C., Perry, J., & Merrill, F.E. (2021). Cosmic ray radiography of a human phantom. *Preprint at arXiv 2106.01542.* https://doi.org/10.48550/arXiv.2106.01542

Nasirpour, M.H., Sharifi, A., Ahmadi, M., et al. (2021). Revealing the relationship between solar activity and COVID-19 and forecasting of possible future viruses using multi-step autoregression (MSAR). *Environmental Science and Pollution Research*, 28, 38074 – 38084. https://link.springer.com/article/10.1007/s11356-021-13249-2

Nickolaenko, A.P., Hayakawa, M. & Koloskov, O. (2025). Impact of solar activity on Schumann resonance: model and experiment. Atmosphere, 16 (6), 648. https://doi.org/10.3390/atmos16060648

NOAA Space Weather Prediction Center (Solar Proton Events Affecting the Earth Environment). https://www.ngdc.noaa.gov/stp/space-weather/interplanetary-data/solar-proton-events/SEP%20page%20code.html

Orlyuk M., Romenets A., & Orlyuk I. (2020). Magnetic fields of the Kyiv underground: ecological aspect. Reports of the National Academy of Sciences of Ukraine, 3 (3), 63-70. DOI:10.15407/dopovidi2020.03.063

Potgieter, M.S. (2013). Solar modulation of cosmic rays. *Living Reviews in Solar Physics*,10, Art. numb. 3. doi: 10.12942/lrsp-2013-3

Qin, J., Celestin, S., & Pasko, V.P. (2012). Low frequency electromagnetic radiation from sprite streamers. *Geophysical Research Letters*, 39(2), Cite ID L22803. doi:10.1029/2012GL053991

Randall, W., & Moos, W.S. (1993). The 11-year cycle in human births. *International Journal of Biometeorology*, 37, 72 – 77. doi:10.1007/BF01214384

Shao, X-M., Jensen, D.P., Ho, C., et al. (2025). 3D Radio Frequency Mapping and Polarization Observations Show Lightning Flashes Were Ignited by Cosmic-Ray Showers. *Journal of Geophysical Research: Atmospheres*, 130(5), 1– 23, e2024JD042549. https://doi.org/10.1029/2024JD042549

Shayer, M., & Ginsburg, D. (2007). Thirty years on - a large anti-Flynn Effect? The Piagetian test volume & heaviness norms 1975–2003. J*ournal of Educational Psychology*, 77, 25 – 41. doi:10.1348/000709906X96987

Shea, M.A., & Smart, D.F. (1990). A summary of major solar proton events. *Solar Physics*, 127, 297–320. https://doi.org/10.1007/BF00152170

Tanaka, H.K.M. (2022). Cosmic time synchronizer (CTS) for wireless and precise time synchronization using extended air showers. *Scientific Reports*, 12, Art. numb. 7078. doi: 10.1038/s41598-022-11104-z

Tanaka, Y.T., Hauakava, M., Habara, Y., et al. (2004). Detection of transient ELF emission caused by the extremely intense cosmic gamma-ray flare of 27 December. *Journal of Educational Psychology*, 38(8), Cite ID L08805. doi: 10.1029/2011GL047008

Tau, G.Z., & Peterson, B.S. (2010). Normal development of brain circuits. *Neuropsychopharmacology Reviews*, 35, 147–168. https://doi.org/10.1038/npp.2009.115

The Official Website of the Nobel Prize. https://www.nobelprize.org/prizes/lists/all-nobel-prizes/

United Nations Scientific Committee on the Effects of Atomic Radiation (2008). Sources and effects of ionizing radiation. New York: United Nations 2010, 4, ISBN 978-92-1-142274-0.

Vasylyev, V.P., Kalinichenko, A.I., & Vasylyev, S.V. (2004). Attogram dust grains in the solar system. Forming mechanism, properties and dynamics. *Astronomy and Astrophysics*, 415, 781–790. doi:10.1051/0004-6361:20031777

Vinogradov, E.S. (1989). On the physical factors of intelligence. *Questions of Psychology*, 6, 108–114 (In Russian).

Watson, A.A. (2011). The discovery of Cherenkov radiation and its use in the detection of extensive air showers. *Nuclear Physics B - Proceedings Supplements*, 212, 13 –19. doi: 10.1016/j.nuclphysbps.2011.03.003

Yun, S., Kiffer, F.C., Bancroft, G.L., et al. (2024). The longitudinal behavioral effects of acute exposure to galactic cosmic radiation in female C57BL/6J mice: Implications for deep space missions, female crews, and potential antioxidant countermeasures. *Journal of Neurochemistry*, Online Version of Record before inclusion in an issue. https://doi.org/10.1111/jnc.16225

Zenchenko, T.A., & Breus, T.K. (2021). The Possible effect of space weather factors on various physiological systems of the human organism. *Atmosphere*, 12(3), 346. https://doi.org/10.3390/atmos12030346